of the chlorides.[22] Thus, the observed intermediate conformation is a compromise between the optimum bonding situation occurring for an eclipsed conformation and minimum nonbonding steric repulsions between the chloride and nitrogen atoms for the staggered conformation.

Supplementary Material Available: Tables of anisotropic thermal parameters (Table III), H atom coordinates and isotropic thermal parameters (Table IV), bond distances (Table V) and bond angles (Table VI), observed and calculated structure factors (Table VII), and distances of atoms from the phthalocyanine N_4 least-squares plane (Table VIII) (18 pages). Ordering information is given on any current masthead page.

---

(22) C. Mealli and V. L. Goedken, to be submitted for publication.

Contribution from the Department of Chemistry, Purdue University, West Lafayette, Indiana 47907, and Molecular Structure Center, Indiana University, Bloomington, Indiana 47401

Synthesis, Structure, Spectroscopic Properties, and Electrochemical Behavior of Group 4[†] Metal Derivatives Containing Bulky Aryloxide Ligands[1]

STANLEY L. LATESKY,[‡] JUDY KEDDINGTON,[‡] ANNE K. McMULLEN,[‡] IAN P. ROTHWELL,*[‡] and JOHN C. HUFFMAN[§]

Use of the sterically demanding ligand 2,6-di-*tert*-butylphenoxide (OAr′) allows the isolation of a number of mononuclear, mixed halo–aryloxides of titanium, zirconium, and hafnium. The products can be grouped into three types. The dihalides $Ti(OAr′)_2X_2$ (X = Cl, Br) are deep red solids extremely soluble in all hydrocarbon solvents. Molecular weight measurements indicate a monomeric structure in benzene. The monohalides $M(OAr′)_3Cl$ (M = Ti, Zr, Hf) and $Ti(OAr′)_3X$ (X = Br, I) are monomeric in solution, and ^1H NMR data show that restricted rotation about the M–O–Ar′ bonds occur, leading to nonequivalent *tert*-butyl groups at low temperature. X-ray diffraction studies on $HfCl(OAr′)_3$ and $TiI(OAr′)_3$ show the compounds to be isostructural with an extremely congested metal coordination sphere. The paramagnetic, blue complex $Ti(OAr′)_3$ can be obtained in good yield from $TiCl_3(NMe_3)_2$ and excess $LiOAr′$ in benzene. Crystal data for $HfCl(OAr′)_3$ at −165 °C: $a = 17.521$ (5) Å, $b = 11.155$ (2) Å, $c = 10.686$ (2) Å, $\alpha = 104.71$ (1)°, $\beta = 99.51$ (1)°, $\gamma = 83.82$ (1)°, $Z = 2$, and $d_{calcd} = 1.387$ g cm^{-3} in space group $P\bar{1}$. Crystal data for $TiI(OAr′)_3$ at −164 °C: $a = 17.327$ (8) Å, $b = 11.088$ (5) Å, $c = 10.928$ (4) Å, $\alpha = 106.09$ (2)°, $\beta = 100.29$ (2)°, $\gamma = 82.54$ (2)°, $Z = 2$, and $d_{calcd} = 1.328$ g cm^{-3} in space group $P\bar{1}$. An investigation of the electrochemistry of these compounds shows that the dihalides $Ti(OAr′)_2X_2$ (X = Cl, Br) undergo reversible one-electron reductions to the corresponding monoanions while for the more sterically crowded $Ti(OAr′)_3X$ (X = Cl, Br, I) reduction products are halide dependent.

Introduction

The use of sterically bulky ligands has made considerable impact on a number of important areas of inorganic and organometallic chemistry. The importance of the size of tertiary phosphines (as quantified by cone angles) on a number of stoichiometric and catalytic reactions has been well documented,[2] while the use of the large C_5Me_5 ligand has recently led to the development of novel chemistry in a number of areas.[3–7] Early work by Bradley and others showed that use of bulky ligands such as the bis(trimethylsilyl)amide group can allow the isolation of complexes with unusually low coordination numbers,[8] such complexes giving insight into the electronic structures of transition-metal complexes.[9]

We and others have recently been focusing our attention on the chemistry associated with sterically bulky oxygen donor ligands, and in particular we have been systematically investigating the use of 2,6-dialkylphenoxides as ancillary ligands:[10–15] There has recently been a renaissance in the study of early-transition-metal alkoxide chemistry prompted by a number of developments. Alkoxide groups have played an important part in the development of the chemistry associated with metal–metal multiple bonds[16] while both theoretical[17] and synthetic[18] studies have shown that such groups are essential for certain organometallic reactions such as olefin metathesis. The structural similarities between transition metal alkoxides and metal oxides has been pointed out,[19] and it has been proposed that the study of their reactivity can give insight into chemistry occurring at catalytic metal oxide surfaces.[20] One important aspect of metal alkoxide chemistry stems from the

ability of the alkoxide ligand to act as either a terminal, doubly, or triply bridging group, allowing ready oligomerization to form condensed systems in which the metal attains a higher coordination number:[21] Somewhat fine control of this in some cases unwanted process can be achieved by the choice of the steric properties of

(1) Chemistry of Sterically Crowded Aryloxide Ligands. 5. Part 4: Chamberlain, L.; Rothwell, I. P.; Huffman, J. C. *Inorg. Chem.* **1984**, *23*, 2575.
(2) Tolman, C. A. *Chem. Rev.* **1977**, *77*, 317.
(3) Janowicz, A. H.; Bergman, R. G. *J. Am. Chem. Soc.* **1982**, *104*, 352.
(4) Hoyano, J. K.; Graham, W. A. G. *J. Am. Chem. Soc.* **1982**, *104*, 3723.
(5) Marks, T. J. *Science (Washington, D.C.)* **1982**, *No. 217*, 989.
(6) Watson, P. L. *J. Am. Chem. Soc.* **1983**, *105*, 6491.
(7) Sanner, R. D.; Manriquez, J. M.; Marsh, R. E.; Bercaw, J. E. *J. Am. Chem. Soc.* **1976**, *98*, 3042.
(8) Alyea, E. C.; Bradley, D. C.; Copperthwaite, R. G. *J. Chem. Soc., Dalton Trans.* **1972**, 1580.
(9) Alyea, E. C.; Bradley, D. C.; Copperthwaite, R. G. *J. Chem. Soc., Dalton Trans.* **1973**, 185.
(10) Chamberlain, L.; Keddington, J.; Rothwell, I. P. *Organometallics* **1982**, *1*, 1098.
(11) Chamberlain, L.; Keddington, J.; Huffman, J. C.; Rothwell, I. P. *Organometallics* **1982**, *1*, 1538.
(12) (a) Chamberlain, L.; Rothwell, I. P.; Huffman, J. C. *J. Am. Chem. Soc.* **1982**, *104*, 7338. (b) Chamberlain, L.; Rothwell, I. P. *J. Am. Chem. Soc.* **1983**, *105*, 1665.
(13) (a) Coffindaffer, T.; Rothwell, I. P.; Huffman, J. C. *Inorg. Chem.* **1983**, *22*, 2906. (b) Coffindaffer, T.; Rothwell, I. P.; Huffman, J. C. *Inorg. Chem.* **1983**, *22*, 3178.
(14) Lubben, T. V.; Wolczanski, P. T.; Van Duyne, G. D. *Organometallics* **1984**, *3*, 977.
(15) Hvoslef, J.; Hope, H.; Murray, B. D.; Power, P. P. *J. Chem. Soc., Chem. Commun.* **1983**, 1438.
(16) Cotton, F. A.; Walton, R. A. "Multiple Bonds Between Metal Atoms"; Wiley-Interscience: New York, 1982.
(17) Rappe, A. K.; Goddard, W. A., III *J. Am. Chem. Soc.* **1982**, *104*, 448.
(18) Schrock, R. R. *ACS Symp. Ser.*
(19) Chisholm, M. H. *Polyhedron* **1983**, *2*, 681.
(20) Chisholm, M. H.; Folting, K.; Huffman, J. C.; Rothwell, I. P. *J. Am. Chem. Soc.* **1982**, *104*, 4839.
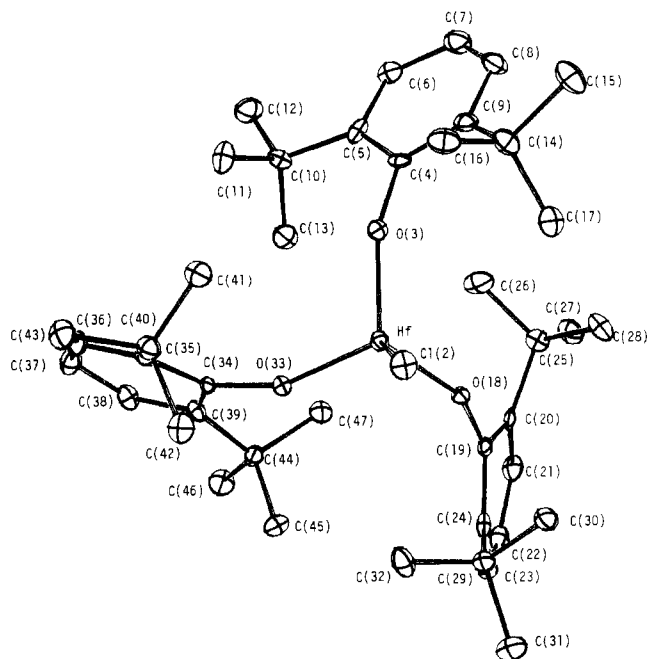(21) Bradley, D. C.; Mehrotra, R. C.; Gaur, D. P. "Metal Alkoxides"; Academic Press: New York, 1978.

Figure 1. ORTEP view of HfCl(OAr′)₃ looking down the Cl–Hf bond.

the alkoxide group, the typical choices being OMe, OEt, OCH₂CMe₃, O-*i*-Pr, and O-*t*-Bu. The ligand 2,6-di-*tert*-butyl phenoxide represents an extremely bulky oxygen donor ligand, and we report here our investigation of the effects this ligand has on the structural, spectroscopic, and electrochemical characteristics of the group 4 metals Ti, Zr, and Hf.[22]

Synthesis of Compounds

The method used for the introduction of the sterically crowded 2,6-di-*tert*-butylphenoxo (OAr′) ligand was metathetic exchange between metal halides and LiOAr′ in hydrocarbon solvent. The addition of the parent phenol (HOAr′) to the metal halides proved unsatisfactory, generating mixtures of products difficult to purify and separate from free phenol. Treatment of the tetrachlorides MCl₄ (M = Zr, Hf) with LiOAr′ (>3 equiv) yielded the compounds M(OAr′)₃Cl [M = Zr (**1**), Hf (**2**)] as pale yellow and white crystalline solids, respectively. All attempts to isolate the disubstituted species M(OAr′)₂Cl₂ either by use of only 2 equiv of LiOAr′ or by mixing M(OAr′)₃Cl with MCl₄ failed. Attempts to substitute the final chloride of **1** and **2** with LiOAr′ in refluxing toluene also proved fruitless. In contrast, use of TiX₄ (X = Cl, Br) with excess of LiOAr′ only yielded the disubstituted complexes Ti(OAr′)₂X₂ [X = Cl (**3**), Br (**4**)] at room temperature as deep red solids. Extended heating with LiOAr′ in toluene did give rise to some of the tris(aryloxide) monohalide but this proved to be an unsatisfactory method of synthesis (vide infra).

The use by Bradley of a number of sterically bulky dialkylamide ligands allowed the isolation of the first series of three-coordinate, mononuclear complexes of transition metals.[8] Treatment of TiCl₃(THF)₃ with LiOAr′ failed to give a reaction in THF after 24 h. However, with TiCl₃(HNMe₂)₂ in benzene the deep blue, extremely air- and moisture-sensitive complex Ti(OAr′)₃ (**5**) could be isolated in good yield. The ease of oxidation of **5** was used synthetically, allowing the ready formation of the monohalides Ti(OAr′)₃X [X = Cl (**6**), Br (**7**), I (**8**)] by treatment with CX₄ (X = Cl, Br) or I₂ in benzene. Iodine reacted rapidly with **5**, giving a deep red solution in hexane whereas the carbon tetrahalides reacted over 12 h at 25 °C, yielding red-orange solutions. All three complexes could be readily recrystallized from hexane.

Molecular Structure

All compounds (**1–8**) gave parent molecular ions in their mass spectra along with fragments due to (M – OAr′)⁺ and (M – X)⁺

(22) Chamberlain, L.; Keddington, J.; Huffman, J. C.; Rothwell, I. P. *J. Chem. Soc., Chem. Commun.* **1982**, 805.

Table I. Crystallographic Data for Compounds **2** and **8**

	2	8
formula	HfClO₃C₄₂H₆₉	TiIO₃C₄₂H₆₉
fw	829.90	7̲90.76
space group	P1̄	P1̄
a, Å	17.521 (5)	17.327 (8)
b, Å	11.155 (2)	11.088 (5)
c, Å	10.686 (2)	10.928 (4)
α, deg	104.71 (1)	106.09 (2)
β, deg	99.51 (1)	100.29 (2)
γ, deg	83.82 (1)	82.54 (2)
Z	2	2
V, Å³	1987.67	1977.81
d(calcd), g/cm³	1.387	1.328
cryst size, mm	a	0.10 × 0.09 × 0.09
cryst color	colorless	yellow
radiation	Mo Kα (λ = 0.710 69 Å)	
linear abs coeff, cm⁻¹	27.018	10.197
temp, °C	−165	−164
detector aperture	3.0 mm wide × 4.0 mm high; 22.5 cm from cryst	
sample to source dist, cm	23.5	23.5
takeoff angle, deg	2.0	
scan speed, deg/min	4.0	
scan width, deg	2.0 + 0.692 tan θ	
bkgd counts, s	5	10
2θ range, deg	5–50	6–45
no. of data collcd	5304	5771
no. of unique data	5213	5186
no. of unique data with $F_o > 2.33\sigma(F)$	4821	4454[b]
R(F)	0.0235	0.0456
Rw(F)	0.0251	0.0467
goodness of fit	0.892	1.014
largest Δ/σ	0.05	0.05

[a] Crystal dimensions (hkl, d, mm): −1,1,0, 0.0600; 1,−1,0, 0.0600; 100, 0.0880; −1,0,0, 0.0880; 110, 0.0950; −1,−1,0, 0.0950; 0, −1,1, 0.1000; 0,1,−1, 0.1000; −1,0,1, 0.1350; 1,0,−1, 0.1350. [b] Unique intensities with $F_o > 3.00\sigma(F)$.
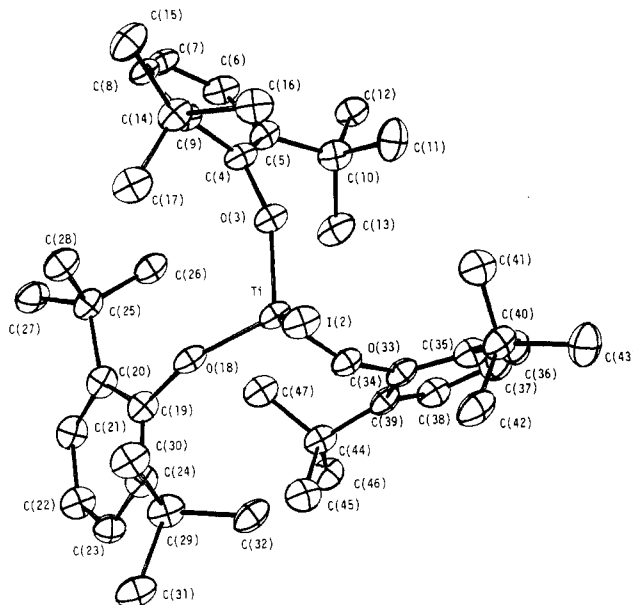

Figure 2. ORTEP view of TiI(OAr′)₃ looking down the I–Ti bond. The opposite enantiomer from that in Figure 1 is shown.

However, the observation of only mononuclear ions does not rule out the presence of oligomers in condensed phase, a property typical of early-transition-metal alkoxides.[21] In order to obtain accurate data concerning the coordination properties of these aryl oxides, the X-ray crystal structures of **2** and **8** were determined. These and the other compounds can be grouped into three categories.

1. Monohalides M(OAr′)₃X (1, 2, and 6–8). These species we believe to be isostructural. The solid-state structures of the iso-

Table II. Fractional Coordinates and Isotropic Thermal Parameters for HfCl(OAr')₃ (2)

atom	10^4x	10^4y	10^4z	$10B_{iso}$, A²
Hf(1)	2399.8 (1)	2020.4 (1)	1478.0 (2)	9
Cl(2)	1963 (1)	3161 (1)	−123 (1)	14
O(3)	3524 (1)	1874 (2)	1765 (2)	10
C(4)	4276 (2)	2035 (4)	2400 (4)	10
C(5)	4720 (2)	1031 (4)	2809 (4)	12
C(6)	5406 (2)	1313 (4)	3653 (4)	15
C(7)	5655 (2)	2498 (4)	4047 (4)	20
C(8)	5256 (2)	3419 (4)	3505 (4)	17
C(9)	4571 (2)	3207 (4)	2628 (4)	12
C(10)	4498 (2)	−334 (4)	2345 (4)	12
C(11)	3778 (2)	−511 (4)	2892 (4)	17
C(12)	5152 (2)	−1222 (4)	2816 (5)	20
C(13)	4359 (3)	−722 (4)	851 (4)	19
C(14)	4193 (2)	4216 (4)	1936 (4)	16
C(15)	4723 (3)	5287 (4)	2146 (5)	23
C(16)	4055 (2)	3676 (4)	444 (4)	17
C(17)	3448 (2)	4813 (4)	2467 (4)	16
O(18)	1926 (1)	2939 (2)	2970 (2)	8
C(19)	1474 (2)	3021 (3)	3949 (4)	10
C(20)	1848 (2)	3020 (3)	5223 (4)	11
C(21)	1399 (2)	2767 (4)	6062 (4)	14
C(22)	620 (3)	2600 (4)	5701 (4)	18
C(23)	253 (2)	2833 (4)	4535 (4)	15
C(24)	661 (2)	3103 (3)	3637 (4)	12
C(25)	2686 (2)	3406 (4)	5702 (4)	13
C(26)	2895 (2)	3555 (4)	7182 (4)	18
C(27)	3295 (2)	2488 (4)	5070 (4)	20
C(28)	2714 (3)	4707 (4)	5454 (4)	19
C(29)	232 (2)	3561 (4)	2448 (4)	15
C(30)	210 (2)	2579 (4)	1159 (4)	17
C(31)	−621 (2)	3990 (4)	2637 (5)	22
C(32)	600 (2)	4730 (4)	2365 (4)	16
O(33)	2010 (1)	401 (2)	870 (2)	10
C(34)	2059 (2)	−887 (3)	476 (4)	9
C(35)	2266 (2)	−1452 (4)	−776 (4)	10
C(36)	2461 (2)	−2722 (4)	−1033 (4)	14
C(37)	2400 (2)	−3416 (4)	−159 (4)	16
C(38)	2086 (2)	−2854 (4)	963 (4)	14
C(39)	1898 (2)	−1578 (4)	1319 (4)	11
C(40)	2218 (2)	−752 (4)	−1867 (4)	13
C(41)	2876 (2)	107 (4)	−1643 (4)	15
C(42)	1418 (2)	−55 (4)	−2013 (4)	16
C(43)	2286 (2)	−1665 (4)	−3200 (4)	16
C(44)	1488 (2)	−1022 (4)	2530 (4)	11
C(45)	714 (2)	−346 (4)	2104 (4)	17
C(46)	1286 (3)	−2042 (4)	3146 (4)	18
C(47)	1977 (2)	−150 (4)	3624 (4)	14

Table III. Fractional Coordinates and Isotropic Thermal Parameters for TiI(OAr')₃ (8)

atom	10^4x	10^4y	10^4z	$10B_{iso}$, A²
Ti(1)	2359 (1)	1966 (1)	1495 (1)	18
I(2)	1820.5 (2)	3322.7 (4)	−158.4 (4)	24
O(3)	3423 (2)	1873 (3)	1745 (4)	22
C(4)	4195 (3)	1994 (6)	2400 (6)	24
C(5)	4624 (3)	947 (6)	2752 (6)	24
C(6)	5295 (4)	1211 (6)	3670 (6)	29
C(7)	5555 (4)	2393 (7)	4145 (7)	34
C(8)	5181 (4)	3323 (6)	3605 (7)	32
C(9)	4507 (4)	3166 (6)	2676 (6)	26
C(10)	4432 (3)	−420 (5)	2193 (6)	24
C(11)	3725 (4)	−663 (6)	2716 (6)	28
C(12)	5107 (4)	−1347 (6)	2542 (7)	30
C(13)	4259 (4)	−734 (6)	733 (7)	30
C(14)	4184 (4)	4177 (6)	1956 (6)	28
C(15)	4798 (5)	5134 (7)	2185 (7)	40
C(16)	4053 (4)	3590 (6)	513 (7)	33
C(17)	3455 (4)	4918 (6)	2461 (6)	30
O(18)	1909 (2)	2805 (3)	2890 (4)	21
C(19)	1482 (3)	2925 (5)	3885 (6)	22
C(20)	1896 (3)	2909 (5)	5124 (6)	22
C(21)	1462 (4)	2645 (6)	5973 (6)	26
C(22)	675 (4)	2510 (6)	5653 (6)	26
C(23)	270 (3)	2764 (6)	4533 (6)	24
C(24)	648 (3)	3044 (5)	3633 (5)	22
C(25)	2745 (4)	3258 (6)	5582 (6)	27
C(26)	2972 (4)	3499 (6)	7054 (6)	27
C(27)	3328 (4)	2225 (7)	4979 (6)	32
C(28)	2814 (4)	4489 (7)	5272 (7)	34
C(29)	174 (3)	3605 (5)	2553 (6)	23
C(30)	88 (4)	2669 (6)	1219 (6)	26
C(31)	−665 (4)	4077 (6)	2840 (7)	29
C(32)	555 (4)	4760 (6)	2529 (6)	25
O(33)	2016 (2)	444 (4)	780 (4)	22
C(34)	2053 (3)	−846 (5)	323 (6)	22
C(35)	2300 (3)	−1414 (5)	−897 (6)	24
C(36)	2535 (4)	−2697 (6)	−1169 (6)	24
C(37)	2467 (4)	−3390 (6)	−322 (6)	29
C(38)	2115 (4)	−2845 (6)	756 (6)	26
C(39)	1891 (3)	−1578 (6)	1118 (6)	23
C(40)	2235 (4)	−730 (5)	−1978 (5)	24
C(41)	2879 (4)	151 (6)	−1741 (6)	26
C(42)	1409 (4)	−47 (6)	−2115 (6)	28
C(43)	2304 (4)	−1666 (6)	−3291 (6)	28
C(44)	1440 (3)	−1043 (5)	2283 (6)	23
C(45)	682 (4)	−277 (6)	1861 (7)	30
C(46)	1186 (4)	−2091 (6)	2739 (7)	32
C(47)	1926 (4)	−240 (6)	3446 (6)	27

morphs Hf(OAr')₃Cl (**2**) and Ti(OAr')₃I (**8**) are shown in Figures 1 and 2. Table I gives the crystallographic data while Tables II and III give the fractional coordinates and isotropic thermal parameters. Tables IV and V give selected bond distances and angles. In both compounds the metal occupies a tetrahedral environment surrounded by three oxygens and a halide donor atom with some distortions due to the steric bulk of the aryloxide ligand. The X–M–O angles are compressed slightly to 107.4 (average) and 105.7° (average) for **2** and **8** while the O–M–O angles open up to 111.5 (average) and 112.7° (average), respectively. This steric pressure both at the metal center and between adjacent aryl oxides is partially relieved by the following effects. In both compounds the M–O–Ar' angles are large, 155.7 (average) (**2**) and 157.4° (average) (**8**). This has the effect of relieving interactions between the *tert*-butyl groups of the aryloxide and the metal as well as with other substituents and is a common feature of this and other aryloxide ligands. Although there is a large steric component to the opening up of this angle, it also reflects to a certain degree the amount of oxygen p to metal d π bonding that is taking place at these electron-deficient, d⁰ metal centers. In the extreme case it is possible to envisage a total of six electrons being donated by an aryloxide ligand, assuming the availability of metal orbitals of the correct symmetry. The short Hf–O and Ti–O distances of 1.93 (average) and 1.79 Å (average) also clearly

Table IV. Selected Bond Distances (Å) and Angles (deg) for HfCl(OAr')₃ (2)

	Distances		
Hf(1)–Cl(2)	2.365 (1)	Hf(1)–O(18)	1.925 (2)
Hf(1)–O(3)	1.938 (3)	Hf(1)–O(33)	1.917 (3)

	Angles		
Cl(2)–Hf–O(3)	109.5 (1)	O(18)–Hf–O(33)	109.7 (1)
Cl(2)–Hf–O(18)	103.9 (1)	Hf–O(3)–C(4)	159.4 (2)
Cl(2)–Hf–O(33)	108.8 (1)	Hf–O(18)–C(19)	152.0 (2)
O(3)–Hf–O(18)	114.9 (1)	Hf–O(33)–C(34)	155.9 (2)
O(3)–Hf–O(33)	109.9 (1)		

Table V. Selected Bond Distances (Å) and Angles (deg) for TiI(OAr')₃ (8)

	Distances		
Ti(1)–I(2)	2.634 (8)	Ti(1)–O(18)	1.802 (7)
Ti(1)–O(3)	1.810 (9)	Ti(1)–O(33)	1.782 (8)

	Angles		
I(2)–Ti–O(3)	108.6 (2)	O(18)–Ti–O(33)	112.6 (3)
I(2)–Ti–O(18)	102.9 (3)	Ti–O(3)–C(4)	159.1 (4)
I(2)–Ti–O(33)	106.4 (3)	Ti–O(18)–C(19)	155.2 (4)
O(3)–Ti–O(18)	114.9 (3)	Ti–O(33)–C(34)	158.2 (4)
O(3)–Ti–O(33)	110.7 (3)		

reflect the presence of considerable multiple bonding between these groups. The dramatic difference between these two distances also highlights the much more crowded metal environment generated in the titanium complexes compared to analogous ones of zirconium and hafnium, a fact almost certainly responsible for the more sluggish substitution that occurs with the first-row element.

The almost linear M–O–Ar′ angle allows one to consider the steric properties of the OAr′ ligands to be similar to a propeller occupying a "wedgelike" piece of the metal coordination sphere. This is similar to the analogies drawn for dialkylamido ligands. The plane of this wedge in 2,6-dialkylphenoxides is defined by the plane of the aryl ring. In the structures we and others have determined on 2,6-dialkylphenoxides coordinated to transition metals, the plane of the aryl ring is always close to perpendicular to the plane defined by the M–O–C(Ar) atoms. This is not surprising as it allows, for these symmetrical ligands, the bulky alkyl groups to become equidistant from the metal. If these two planes lie parallel, then steric pressure between one of the alkyl groups and the metal is maximized. In both compounds 2 and 8 the three wedges orient themselves in a similar fashion, lying at an angle of $24 \pm 2°$ to the M–X axis. This results in there being two types of *tert*-butyl groups, those proximal to the halide and those distal. This tilting of the aryloxide planes is clearly a compromise in order to help reduce the steric congestion caused by the distal *t*-Bu groups that occupy the space trans to the M–X group.

Another effect that one might expect to see in order to relieve steric strain is a lengthening of the M–X bond caused by a squeezing of the halide by the proximal *t*-Bu groups. It is difficult to accurately evaluate the Ti–I distance, as only one other structure containing this function has even been reported previously.[23] However, both this and the Hf–Cl distance in 2 do not appear to be lengthened to any significant extent. In the infrared spectra of M(OAr′)₃Cl [M = Ti (6), Zr (1), Hf (2)], bands at 425, 372, and 354 cm⁻¹ can be assigned to the M–Cl stretch, while slightly weaker bands at 480, 465, and 460 cm⁻¹ can be assigned to the antisymmetric MO₃ stretching vibration. The higher values of $\bar{\nu}$(M–Cl) compared to the related series of compounds ClM[N-(SiMe₃)₃]₃[24] correlates well with the shorter Hf–Cl distance in 2 compared to those in the hafnium amide complex. This lengthening with the amido coligands may be due to the better π-donor properties of this ligand, competing for metal orbitals that are used in M–Cl bonding.

2. Dihalides Ti(OAr′)₂X₂ (3 and 4). The simple phenoxide Ti(OPh)₂Cl₂ has been shown to be a dimer in the solid state with two bridging phenoxo groups.[25] Despite initial reports to the contrary,[26] it seems that this compound maintains its dimeric nature in benzene solution, and there is evidence for the slowing down of exchange of bridge and terminal OPh resonances in the ¹H NMR spectrum at low temperatures.[27] It is hence of interest to compare the structures of 3 and 4 to see the effect that the bulky OAr′ ligand has on this dimerization process.

Molecular weight measurements on dichloride 3 gave a value of 507 in benzene solution. This is close to the calculated value of 523 expected for a monomer. Similarly, although there was a general broadening, ¹H NMR spectra of both 3 and 4 showed only one *t*-Bu environment in CDCl₃ solutions down to –60 °C. Hence, unlike the simple phenoxide, the presence of the bulky OAr′ ligand has favored a monomeric structure in solution.

3. Triphenoxide Ti(OAr′)₃ (5). The deep blue complex 5 unfortunately did not give crystals suitable for X-ray analysis. However, recent results by Lappert et al. include the structure of the related compound [Sc(OAr′-4-Me)₃] (OAr′-4-Me = 4-
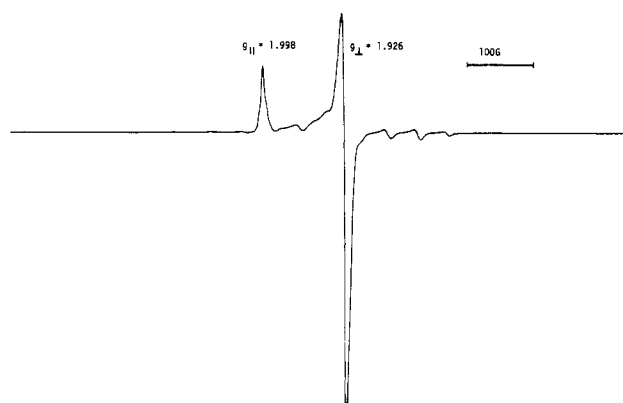
(23) Clark, R. J. H. In "Comprehensive Inorganic Chemistry"; Pergamon Press: New York, 1973.
(24) Airoldi, C.; Bradley, D. C.; Chudzynska, H.; Hursthouse, M. B.; Abdul-Malik, K. M.; Praithby, P. R. *J. Chem. Soc., Dalton Trans.* **1980**, 2010.
(25) Wautenpaugh, K.; Caughlan, C. N. *Inorg. Chem.* **1966**, *5*, 1782.
(26) Frazer, M. J.; Goffes, Z. *J. Inorg. Nucl. Chem.* **1966**, *28*, 2410.
(27) Flamini, A.; Cole-Hamilton, D. J.; Wilkinson, G. *J. Chem. Soc., Dalton Trans.* **1978**, 454.

Figure 3. X-Band EPR spectrum of Ti(OAr′)₃ in frozen toluene.

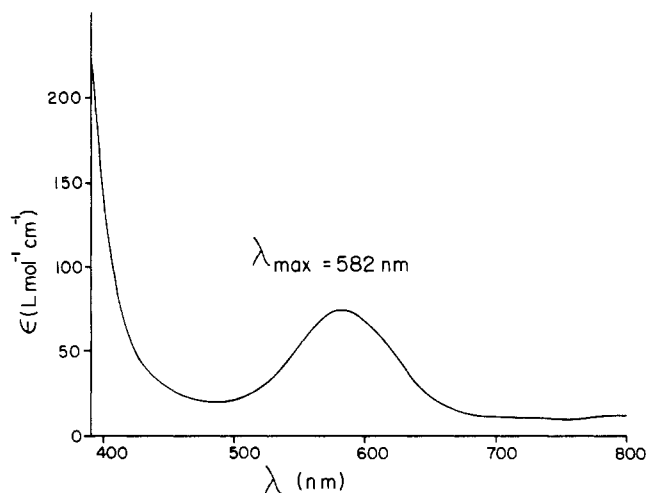**Figure 4.** Absorption spectrum of Ti(OAr′)₃ in cyclohexane solvent.

methyl-2,6-di-*tert*-butylphenoxide).[28]   In the solid state the complex is mononuclear with an approximately trigonal-planar MO₃ skeleton. There is every reason to expect 5 to adopt an analogous structure. Solutions of 5 exhibit a strong ESR signal at room temperature with the expected ⁴⁷Ti ($I = ^7/_2$) and ⁴⁹Ti ($I = ^5/_2$) satellites. The frozen spectrum is shown (Figure 3) and allows the measurement of $g_{\parallel}$ and $g_{\perp}$ for this complex. Study of the ESR and electronic absorption spectrum of the complex Ti[N(SiMe₃)₂]₃ allowed Bradley et al. to assign a value to the spin–orbit coupling constant in this complex.[9] It would be of interest to compare the values of these constants on going from a nitrogen to an oxygen environment about the Ti(III) center. However, a problem arises. In the electronic spectrum of the silylamide two absorptions were measured, one of medium intensity at 17 400 cm⁻¹ and a much weaker absorption at 4800 cm⁻¹. In a D_{3h} field the metal d orbitals should split into three sets, a′₁ (d_{z²}), ϵ'' (d_{xz}, d_{yz}), and ϵ' (d_{xy}, d_{x²-y²}). The unpaired electron on titanium should hence lie in the lowest lying, nondegenerate d_{z²} orbital giving rise to an $^2A'_1$ ground state. The two transitions were assigned as the symmetry-allowed $^2A'_1 \rightarrow$ $^2E'$ and symmetry-forbidden $^2A'_1 \rightarrow$ $^2E''$ transitions, respectively. The relatively small energy for the $^2A'_1 \rightarrow$ $^2E''$ transition reflects the similarity in energy of the d_{z²} and d_{xz}, d_{yz} sets of orbitals in this ligand field. In the case of complex 5 the higher ligand field transition is readily measured at 582 nm (17 200 cm⁻¹) very close to the value for the silylamide complex (Figure 4). However, we have been unable, using a variety of instruments, to observe the lower energy absorption band for 5. Comparison of the *g* values for 5 and Ti[N(SiMe₃)₂]₃ (parentheses) shows a significant difference in the values of $g_{\perp}$: $g_0 = 1.947$ (1.911), $g_{\parallel} = 1.998$ (1.993), $g_{\perp} = 1.926$ (1.869). The theory for *g* values predicts $g_{\parallel} = 2$ and $g_{\perp} = 2(1 - 3\zeta/\Delta)$ where

(28) Hitchcock, P. B.; Lappert, M. F.; Singh, A. *J. Chem. Soc., Chem. Commun.* **1983**, 1499.

Table VI. ^{1}H NMR Data for Compounds $M(OAr')_3X^a$

complex	δ(CMe$_3$)	Δ, Hz	T_c, K	E_a
1	1.15 (s)	58	233	10.7
	1.80 (s, b)			
2	1.15 (s)	57	233	10.8
	1.78 (s, b)			
6	1.25 (s)	54	265	12.3
	1.85 (s, b)			
7	1.20 (s)	58	268	12.4
	1.85 (s, br)			
8	1.20 (s)	67	268	12.3
	1.95 (s, b)			

^{a} E_a in kcal mol^{-1} based on T_c; Δ measured at 90 MHz; separation of proximal and distal CMe$_3$ groups at −65 °C in toluene-d_8.

ζ is the spin–orbit coupling parameter and Δ is the energy difference between the $^2A'_1$ ground state and the $^2E''$ excited state. With the data available Bradley was able to fit the value of $g_\perp$ to theory if the spin–orbit coupling constant was reduced to 70% of the free-ion value of 154 cm^{-1}. Accepting the lack of data concerning the value of Δ, we can only conclude that the ratio of ζ/Δ is 0.0655 for complex **5**. However, assuming the maximum value for h of 154 cm^{-1} (i.e., the free-ion value), then one finds a predicted value of Δ of 2350 cm^{-1}. The quenching of spin–orbit coupling by the aryloxide ligands will have the effect of decreasing this value. Hence, we can conclude that the separation of the a$'_1$ and ϵ' sets of orbitals is less than 2350 cm^{-1} compared to 4800 cm^{-1} in the silylamide complex. This absorption band is therefore predicted to occur in the infrared part of the spectrum of complex **5**. We have been unable to observe such a band.

The decrease in the separation of the two lowest sets of orbitals on going from N(SiMe$_3$)$_2$ to OAr' as coligands may be rationalized in terms of π-bonding effects. Under D_3 symmetry (the correct symmetry for the silylamide in the solid state) the filled p$_z$ orbitals on the amide nitrogen atoms have the correct symmetry (a$_2$ + ϵ) to interact with both of the d$_{xz}$,d$_{yz}$ and d$_{xy}$,d$_{x^2-y^2}$ sets of metal orbitals. This will effectively push them up in energy and could explain the observed increase in the $^2A' \rightarrow {}^2E'$ transition, the amide ligands being much better π donors than the aryloxides.

Fluxional Behavior of M(OAr')$_3$X Type Compounds

The ^{1}H NMR data for all of the monohalide compounds is given in Table VI. At room temperature the aryloxide ligands give rise in all cases to a single t-Bu resonance between δ 1.4 and 1.7 and the expected aromatic multiplets between δ 6.6 and 7.0. As discussed earlier, the solid-state structure of the monohalides **2** and **8** show that the aryloxide ligands should be equivalent in the molecule, virtual C_3 symmetry, but that the orientation of the aryl groups is such that two types of t-Bu groups are present. The presence of only one single resonance for the group implies that exchange of proximal and distal t-Bu groups is facile at this temperature, representing rotation about the M–O–Ar' bonds. After the solutions of these complexes are cooled, the ^{1}H NMR spectrum changes. The t-Bu signal begins to broaden and separates out into two equal-intensity broad signals. This hence represents the "freezing-out" of rotation about the M–O–Ar' bonds on the NMR time scale. One would then expect that on further cooling both of these signals would sharpen up to give a limiting spectrum consisting of two sharp singlets for the proximal and distal t-Bu groups. However, the situation becomes slightly more complex. On further cooling, only one of the resonances begins to sharpen up; the other one begins to broaden even further. At the lowest temperature we have been able to achieve, the higher field signal is relatively sharp but the lower field signal begins to broaden out and some structure is beginning to appear. We interpret these data in terms of two fluxional processes occurring. First, there is restricted rotation about the M–O–Ar' bonds due to the steric influence of the bulky OAr' groups, and then at lower temperatures one of the t-Bu groups is itself undergoing restricted rotation. Analysis of the structures in Figures 1 and 2 leads us to conclude that it is the proximal t-Bu groups that are responsible
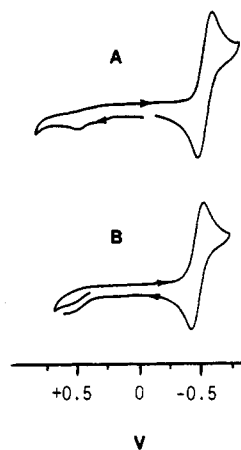

Figure 5. Cyclic voltammograms of Ti(OAr')$_2$X$_2$, X = Cl (A), and Br (B), in THF/TBAH in volts vs. a Ag/AgCl pseudoreference electrode. Scan rates are 25 mV/s.

Table VII. Electrochemical and ESR Data

complex	$E_{1/2}$,^{a}	g^b	complex	$E_{1/2}$,^{a} V
Ti(OAr')$_2$Cl$_2$ (3)	−0.50	1.9384	Ti(OAr')$_3$Br (7)	−0.95^c
Ti(OAr')$_2$Br$_2$ (4)	−1.00	1.9603	Ti(OAr')$_3$I (8)	−0.80^c
Ti(OAr')$_3$Cl (6)	−1.00			

^{a} Potentials measured at 25 mV/s scan rate vs. Ag/AgCl pseudoreference electrode in THF/0.2 M TBAH. ^{b} g value of one-electron-reduced complex, if observed, in THF taken from the X-band ESR spectrum at 30 °C. ^{c} Reduction irreversible, $E_{p,c}$ quoted.

for the broader, low-field resonance. The orientation is such that these groups are being forced up against the M–X bond, so that in a static structure they adopt a conformation in which the *tert*-butyl methyl groups are nonequivalent in the ratio of 2:1. In fact, in the solid state with the aryl rings inclined at 24° to the M–X axis, all three would be nonequivalent. However, it seems reasonable that rocking of the aryl groups from +24° to −24° without exchanging proximal and distal t-Bu groups will be very facile. This rocking also has the effect of exchanging the two enantiomers for these molecules; both enantiomers were present in the unit cells of **2** and **8**.

Table VI also lists the activation energy for proximal–distal exchange based on the coalescence temperatures. It can be seen that the barrier to rotation is consistently higher for M = Ti compared to M = Zr and Hf. This is a reflection no doubt of the more crowded coordination sphere for the first-row transition element. However, in the series going from **6** to **8** there appears to be little dependence on the nature of the halide. This implies that it is the bulk of the other OAr' substituents that is a deciding factor for the fluxionality of these molecules.

Electrochemical Studies

We have investigated the electrochemical behavior (cyclic voltammetry, coulometry, preparative electrolysis) of the compounds obtained in this study. In tetrahydrofuran (THF) with Bu$_4$N$^+$PF$_6^-$ (TBAH, 0.2 M) as supporting electrolyte, cyclic voltammetry at a platinum-disk electrode shows for the dihalides Ti(OAr')$_2$X$_2$ [X = Cl (3), Br (4)] a completely reversible and very accessible one-electron reduction (Table VII; Figure 5). The reversibility of the electron transfer was judged by the ratio $i_{p,a}/i_{p,c}$ = 1 for scan rates between 20 and 500 mV/s, with the peak spread of the wave being the same as that of the Cp$_2$Fe$^+$/Cp$_2$Fe couple under identical conditions. Controlled-potential reduction at $E_{p,c}$ of THF/TBAH solutions of these complexes produces, after the passage of one electron, yellow (X = Cl) or green (X = Br) solutions from their initially deep red color. These solutions exhibit cyclic voltammograms identical with those of the initial complexes except that now the observed wave is an oxidation. Strong ESR signals are also observed for both solutions, and in the case of the dibromide coupling to *two* bromine nuclei can be clearly seen
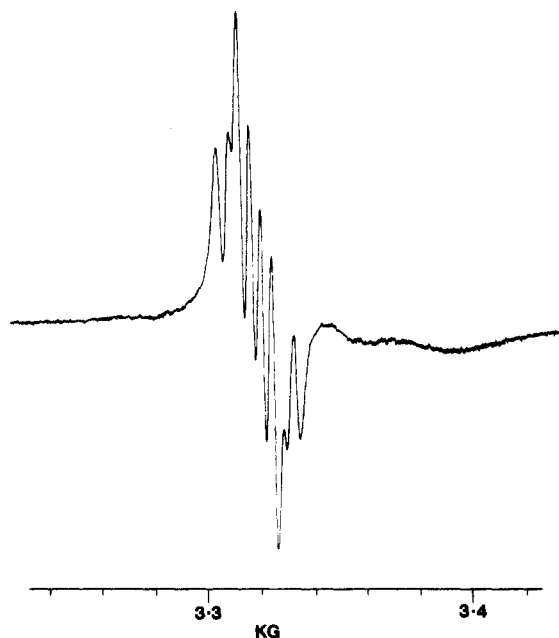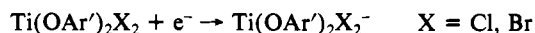
Figure 6. X-Band ESR spectrum of Ti(OAr′)$_2$Br$_2^-$ in THF at -15 °C.

(Figure 6). These observations are consistent with electron transfer to these complexes being completely reversible in THF/TBAH, with no significant halide or aryloxide dissociation taking place.

$$Ti(OAr')_2X_2 + e^- \rightarrow Ti(OAr')_2X_2^- \qquad X = Cl, Br$$

This behavior is similar to that reported for Cp$_2$TiX$_2$ (X = Cl, Br) where, despite initially conflicting reports,[29] it has been shown that the first one-electron reduction is completely reversible as studied by electrochemical methods.[30]

For the more sterically crowded monohalides Ti(OAr′)$_3$X [X = Cl (6), Br (7), I (8)] the electron-transfer behavior is strongly halide dependent. The cyclic voltammograms of these three complexes are shown (Figure 7). The monochloride complex (6) exhibits an electrochemically reversible one-electron reduction, although the peak separation is significantly larger than that of the Cp$_2$Fe/Cp$_2$Fe$^+$ couple under similar conditions. Bulk electrolysis of the red solutions of this complex yield yellow solutions that exhibit almost identical CV's except that the wave is now anodic. However, these solutions exhibit a small (<5%) wave at positions identical with those of authentic samples of Ti(OAr′)$_2$Cl$_2$ (3), indicating that a small amount of ligand exchange has occurred on reduction of the monochloride. In the case of the monobromide (7), the one-electron reduction is completely irreversible, with no significant anodic wave being present at scan rates up to 500mV/s. However, on scanning anodically after passing this reduction, a wave identical with the anodic wave of Ti(OAr′)$_2$Br$_2^-$ and a broad oxidation wave at +0.7 V are observed. This latter wave we have identified as being due to the irreversible oxidation of OAr′$^-$ in THF/TBAH. These results are consistent with an electron-transfer-promoted ligand-rearrangement reaction:

$$2Ti(OAr')_3Br + 2e^- \rightarrow Ti(OAr')_2Br_2^- + OAr^- + [Ti(OAr')_3]$$

Bulk, controlled-potential electrolysis (-0.4 V) of solutions of Ti(OAr′)$_3$Br generated dark greenish solutions whose cyclic voltammogram exhibited two oxidation waves, one due to Ti(OAr′)$_2$Br$_2^-$ and the other due to OAr′$^-$. The cyclic voltammogram of blue solutions of Ti(AOr′)$_3$ (5) in THF/TBAH shows only a very broad, irreversible oxidation wave at $E_{p,a}$ = -0.02 V. This wave could not be identified in the reduced solutions of Ti(OAr′)$_3$Br (7), and hence its existence in this reduced solution

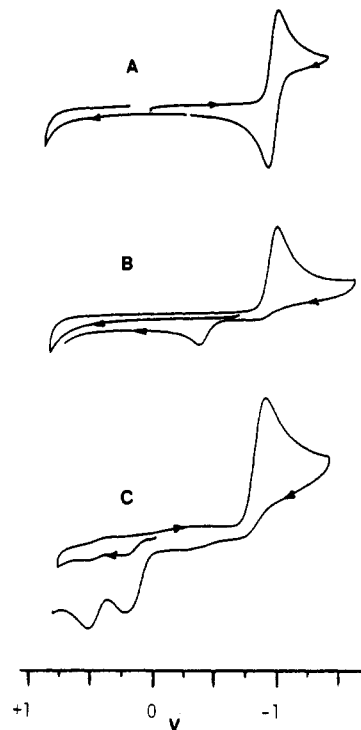(29) El Murr, N.; Chaloyard, A. *J. Organomet. Chem.* **1981**, *212*, C39 and references therein.
(30) El Murr, N.; Chaloyard, A.; Tirouflet, J. *J. Chem. Soc., Chem. Commun.* **1980**, 446.

Figure 7. Cyclic voltammograms of Ti(OAr′)$_3$X, X = Cl (A), Br (B), and I (C), in THF/TBAH in volts vs. a Ag/AgCl pseudoreference electrode. Scan rates are 25 mV/s.

is at present conjecture based on the other products observed.

For the monoiodide, Ti(OAr′)$_3$I (8), an irreversible one-electron reduction is observed that results, on scanning anodic, in the formation of two irreversible oxidation waves at +0.21 and +0.51 V. These two waves are characteristic of iodide ion (I$^-$), confirmed by analysis of Bu$_4$N$^+$I$^-$ added to the supporting electrolyte. Bulk reduction of solutions of Ti(OAr′)$_3$I (8) at $E_{p,c}$ generated a deep green-blue solution whose CV showed not only two oxidation waves due to iodide ion but also a number of other, broad oxidation waves. The EPR spectrum of this solution exhibits a signal with an *g* value identical with that of Ti(OAr′)$_3$ although the signal was weak. Hence, it appears in this case that electron transfer results in rapid dissociation of iodide ion to give Ti(OAr′)$_3$ (5) although other reactions may also be taking place.

$$Ti(OAr')_3I + e^- \rightarrow Ti(OAr')_3 + I^-$$
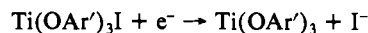
The CV of Zr(OAr′)$_3$Cl (1) shows a very broad, irreversible reduction at $E_{p,c}$ = -1.85 V. Bulk reduction of solutions of 1 at -2.00 V gave intense blue-purple THF/TBAH solutions that exhibited a number of broad CV peaks. The EPR of these solutions showed only broad, ill-resolved resonances. Hence, it appears that reduction of 1 does not lead to simple products, in contrast to the behavior for the titanium complexes.

The experimental results obtained with the series of complexes Ti(OAr′)$_3$X [X = Cl (6), Br (7), I (8)] apparently reflect a steric effect of the halide on the stability of the anions Ti(OAr′)$_3$X$^-$. However, the effect of relative bond strengths and solvation effects are very difficult to evaluate for such systems.

Experimental Section

All manipulations were carried out by using standard techniques to preclude both moisture and oxygen. Analyses were carried out by either Galbraith Microanalytic Service or the internal service at Purdue. Lithium aryloxides were synthesized as described previously.[1]

1. Synthesis of M(OAr′)$_3$Cl [M = Zr (1), Hf (2)]. To a suspension of LiOAr′ (4 equiv) in benzene was added MCl$_4$ from a solid addition funnel at 25 °C. The resulting mixture was stirred for 12 h and filtered and the filtrate stripped under reduced pressure. The resulting solid was suspended in hexane and filtered to remove traces of phenol to give the pure product. Recrystallization of the compounds from hot toluene gave pale yellow (1) and colorless crystals (2). Anal. Calcd for ZrClO$_3$C$_{42}$H$_{63}$ (1): C, 67.93; H, 8.55; Cl, 4.77. Found: C, 66.35; H, 8.02; Cl, 5.44.

Anal. Calcd for HfClO₃C₄₂H₆₃ (**2**): C, 60.79; H, 7.65; Cl, 4.27. Found: C, 60.97; H, 7.60; Cl, 4.48.

2. Synthesis of Ti(OAr′)₂X₂ [X = Cl (3), Br (4)]. The addition of TiX₄ (X = Cl, Br) to a suspension of LiOAr′ (4 equiv) in benzene gave an immediate dark red coloration. After stirring for 12 h, the mixture was filtered and solvent removed from the clear red solution to leave a dark red oil. Analysis by ¹H NMR showed the product plus traces of free 2,6-di-*tert*-butylphenol (HOAr′) as an impurity. The oil was transferred to a round-bottom flask connected to a straight tube sublimer, and the mixture was heated at 70 °C (10⁻³ mm) to remove the more volatile phenol component. On cooling, a dark red solid mass of either **3** or **4** was given. Due to their extreme solubility in hydrocarbon solvents, recrystallization was not possible. Anal. Calcd for TiCl₂O₂C₂₈H₄₂ (**3**): C, 63.52; H, 8.00; Cl, 13.39. Found: C, 63.74; H, 7.95; Cl, 13.13. Anal. Calcd for TiBr₂O₂C₂₈H₄₂: C, 54.43; H, 6.86; Br, 25.84. Found: C, 53.26; H, 6.62; Br, 24.94. ¹H NMR (C₆D₆, 30 °C): (**3**) δ 1.60 (s, *t*-Bu), 7.74 (m, C₆H₃); (**4**) δ 1.55 (s, *t*-Bu), 7.74 (m, C₆H₃).

3. Synthesis of Ti(OAr′)₃ (5). Addition of LiOAr′ (excess) to a blue solution of TiCl₃(HNMe₂)₂ in benzene initially gave a dark green suspension. On stirring for 24 h, a deep blue mixture was given. Solvent was removed under vacuum and the resulting solid mass extracted with cold hexane. After the blue solution was cooled, dark blue plates of product were given.

4. Synthesis of Ti(OAr′)₃X [X = Cl (6), Br (7), I (8)]. To a solution of Ti(OAr′)₃ (**5**) in hexane was condensed CX₄ (X = Cl, Br; 4 equiv) from a calibrated gas manifold. Over a period of a few hours the solution became reddish orange. Cooling to −15 °C gave crystals of product: X = Cl (**6**), Br (**7**). The blue color or a hexane solution of **5** was immediately discharged upon addition of I₂ crystals. Cooling gave crystals of the iodide (**8**). Anal. Calcd for TiClO₃C₄₂H₆₃ (**6**): C, 72.13; H, 9.08; Cl, 5.07. Found: 71.82; H, 9.14; Cl, 5.29. Anal. Calcd for TiBO₃C₄₂H₆₃ (**7**): C, 67.84; H, 8.54; Br, 16.74. Found: C, 67.64; H, 8.62; Br, 10.97. Anal. Calcd for TiIO₃C₄₂H₆₃ (**8**): C, 63.80; H, 8.03; I, 16.05. Found: C, 61.79; H, 8.23; I, 19.05. The unsatisfactory analysis for **8** we believe may be due to some iodination of the aryloxide ligands. However, no evidence of such was seen in the X-ray structure.

X-ray Crystallography. General operating procedures have been reported previously.[31] For both structures the octants collected were +*h*, ±*k*, ±*l*.

(i) HfCl(OAr′)₃ (2). The structure was solved by successive Fourier

syntheses after initially locating the Hf and Cl atoms by a Pattersen function. All atoms, including hydrogens, were located and refined. Hydrogen atoms were assigned isotropic thermal parameters and all other atoms anisotropic thermal parameters. A final difference Fourier synthesis was essentially featureless, the largest peak being 0.35 e/Å³. χ scans were essentially flat, and no absorption correction was performed. The transmission factors for this complex were calculated to range from 0.614 to 0.763 while the effect of secondary extinction in the diffraction data was found to be minimal.

(ii) TiI(OAr′)₃ (8). A systematic search of a limited hemisphere of reciprocal space located a set of diffraction maxima with no systematic absences or symmetry. Statistical tests and the solution and refinement of the structure indicated the proper choice for space group is *P*ī.

The structure was solved by direct methods (MULTAN78) and Fourier techniques and refined by full-matrix least squares. All hydrogen atoms were located and refined (anisotropic for Ti, I, O, and C; isotropic for H). A final difference Fourier was featureless, the largest peak being 0.18 e/Å³. χ scans were essentially flat, and no absorption correction was performed.

Electrochemical Measurements. Cyclic voltammograms were obtained on a BioAnalytical Systems, Inc. Model CV-1A instrument. Potential control for coulometric experiments was performed with a potentiostat purchased from Bio Analytical Systems, Inc. A three-compartment H-cell was used with a Pt-disk or gauze working electrode, Pt-wire auxiliary electrode, and a Ag/AgCl pseudoreference electrode to which all potentials refer. Scan rates were 25 mV/s. Under these conditions the Cp₂Fe/Cp₂Fe⁺ couple was measured at +0.47 V, consistent to ±10 mV, with a separation between the anodic and cathodic waves of 90 mV.

Supplementary Material Available: Listings of anisotropic thermal parameters, complete bond distances and angles, and observed and calculated structure factors (75 pages). Ordering information is given on any current masthead page.

(31) Huffman, J. C.; Lewis, L. N.; Caulton, K. G. *Inorg. Chem.* **1980**, *19*, 2755.

Contribution from the Department of Chemistry,
Louisiana State University, Baton Rouge, Louisiana 70803-1804

"Obstacle Effect" in Palladium(II) Complexes of Tetraamine Ligands with Terminal Pyridyl or Picolyl Residues[1]

GEORGE R. NEWKOME,* YVES A. FRERE,[2] FRANK R. FRONCZEK, and VINOD K. GUPTA

Palladium(II) complexes of several tetraamine ligands with terminal pyridyl or picolyl residues were synthesized, and to ascertain the effect of the 6-methyl group in the microenvironment of the core metal (obstacle effect), single-crystal X-ray analyses on some of the complexes have been conducted. 1,6-Bis(6-methyl-2-pyridyl)-2,5-diazahexane formed 1:2 [Pd(C₁₆H₂₂N₄)₂]Cl₂·3H₂O as well as 1:1 [Pd(C₁₆H₂₂N₄)]Cl₂·3H₂O complexes. Both crystallize in the triclinic space group *P*ī. The unit cell dimensions of the former are *a* = 10.726 (1) Å, *b* = 12.400 (2) Å, and *c* = 15.380 (3) Å with α = 91.36 (1)°, β = 91.48 (1)°, and γ = 112.10 (1)°; *Z* = 2. The latter has *a* = 7.243 (2) Å, *b* = 9.979 (2) Å, and *c* = 15.001 (3) Å with α = 94.68 (2)°, β = 96.20 (2)°, and γ = 103.68 (2)°; *Z* = 2. 1,7-Bis(6-methyl-2-pyridyl)-2,6-diazaheptane formed only the 1:1 complex [Pd(C₁₇H₂₄N₄)]Cl₂·3H₂O, which forms triclinic crystals with space group *P*ī. The unit cell dimensions are *a* = 7.6906 (4) Å, *b* = 10.732 (1) Å, and *c* = 14.114 (5) Å with α = 86.82 (2)°, β = 80.90 (2)°, and γ = 70.52 (1)°; *Z* = 2. In all the complexes there is expected square-planar coordination around the Pd atoms. The salient features in the structure and hydrogen bonding of chloride ions are discussed.

Introduction

Palladium(II) complexes that possess simple N donors are well documented in the literature,[3] and a number of structural studies have been conducted on these complexes.[4] Recently we reported the structural aspects of pyridine[5] or 2,2′-bipyridine[6] Pd(II)

complexes that exhibited an "obstacle effect" as a result of juxtaposed 6-methyl groups. Such an effect has been observed,[7,8] but no structural studies have been made to measure the influence of a 6-alkyl group(s) in pyridine and bipyridine complexes. To

(1) Chemistry of Heterocyclic Compounds. 104. Part 103: Newkome, G. R.; Gupta, V. K.; Pappalardo, S. *Org. Mass Spectrom.* **1984**, *19*, 590.
(2) On leave from Centre de Recherche sur les Macromolecules, Strasbourg, France, 1982–1983.
(3) Hartley, F. R. *Coord. Chem. Rev.* **1981**, *35*, 143.
(4) The Cambridge Crystallographic Files afforded 51 references of structures of Pd(II) complexes with simple N ligands.

(5) Newkome, G. R.; Gupta, V. K.; Fronczek, F. R. *Organometallics* **1982**, *1*, 907 and references therein.
(6) Newkome, G. R.; Fronczek, F. R.; Gupta, V. K.; Puckett, W. E.; Pantaleo, D. C.; Kiefer, G. E. *J. Am. Chem. Soc.* **1982**, *104*, 1782. Newkome, G. R.; Puckett, W. E.; Kiefer, G. E.; Gupta, V. K.; Fronczek, F. R.; Pantaleo, D. C.; McClure, G. L.; Simpson, J. B.; Deutsch, W. A. *Inorg. Chem.* **1985**, *24*, 811.
(7) Goodwin, H. A.; Lions, F. *J. Am. Chem. Soc.* **1960**, *82*, 5013.
(8) Gibson, J. G.; McKenzie, E. D. *J. Chem. Soc. A* **1971**, 1666.